Online September 19, 2024
Journal of Neuroendovascular Therapy 2024; 18: 298–304 DOI: 10.5797/jnet.cr.2024-0015

Case Report

Clinical Features of Intracranial Dural Arteriovenous Fistulas with Spinal Perimedullary Venous Drainage: Report of Two Cases and Literature Review

Katsuya Saito,[1] Go Ikeda,[1] Yoshimitsu Akutsu,[1] Yusuke Morinaga,[1] Shunsuke Kawamoto,[1,2] and Hiroyoshi Akutsu[1]

Objective: We describe two cases of myelopathy onset due to intracranial dural arteriovenous fistulas (DAVFs) and present a literature review.

Case Presentation: (Case 1) A 44-year-old man with subacute onset myelopathy underwent an MRI and DSA. MRI showed T2-hyperintensity from the medulla oblongata to the cervical spinal cord with vascular flow voids, suggestive of a spinal DAVF. Unexpectedly, cerebral angiography revealed a tentorial DAVF. (Case 2) A 47-year-old man with progressive myelopathy underwent a head and spinal MRI. Head MRI and MRA were considered to be normal. Spinal MRI revealed T2-hyperintensity in the cervical spinal cord without obvious vascular flow voids around the spinal cord. Contrast-enhanced MRI showed a patchy gadolinium enhancement in the same spinal cord region with the enhancement of perimedullary vessels. Although myelitis was initially suspected, subsequently spinal DAVF was suspected because cervical CTA revealed abnormal spinal venous drainage. Unexpectedly, cerebral angiography identified a foramen magnum DAVF.

Conclusion: Regarding unexplained cervical myelopathy, even the absence of spinal cord surface vascular flow voids cannot necessarily exclude venous congestive myelopathy due to the DAVFs. In such cases, the contrast-enhanced MRI and cervical CTA are useful for visualizing abnormal vessels around the brain stem and the cervical spine. Especially, the co-presence of the abnormal vessels around the brain stem can suggest the intracranial DAVFs. Not only spinal DAVFs but also intracranial DAVFs should be considered as the differential diagnoses for venous congestive cervical myelopathy, in which cases cerebral angiography including carotid angiography is essential.

Keywords intracranial dural arteriovenous fistula, myelopathy, spinal perimedullary venous drainage, Cognard type V

Introduction

Intracranial dural arteriovenous fistulas (DAVFs) with spinal perimedullary venous drainage are rare diseases. They are classified as Cognard type V DAVFs (CVDFs), and patients often exhibit aggressive behavior.[1–5] CVDFs often present with progressive myelopathy symptoms suggestive of a spinal rather than an intracranial origin. Therefore, initial misdiagnosis often leads to a delay in correct diagnosis and treatment, which can be associated with poor neurological recovery.[3] Here, we describe two case reports of CVDFs and include a literature review.

Case Presentation

Case 1

A 44-year-old man with a 3-week history of subacute progressive tetraparesis, sensory disorders, and bladder dysfunction was referred to our department. Physical examination revealed bilateral motor weakness (manual muscle testing grades 3 and 4) with gait

[1]*Department of Neurosurgery, Dokkyo Medical University, Shimotsugagun, Tochigi, Japan*
[2]*Department of Neurosurgery, Nasu Red Cross Hospital, Otawara, Tochigi, Japan*

Received: February 18, 2024; Accepted: July 18, 2024
Corresponding author: Katsuya Saito. Department of Neurosurgery, Dokkyo Medical University, 880 Kitakobayashi, Mibu, Shimotsugagun, Tochigi 321-0293, Japan
Email: csrbb415@yahoo.co.jp

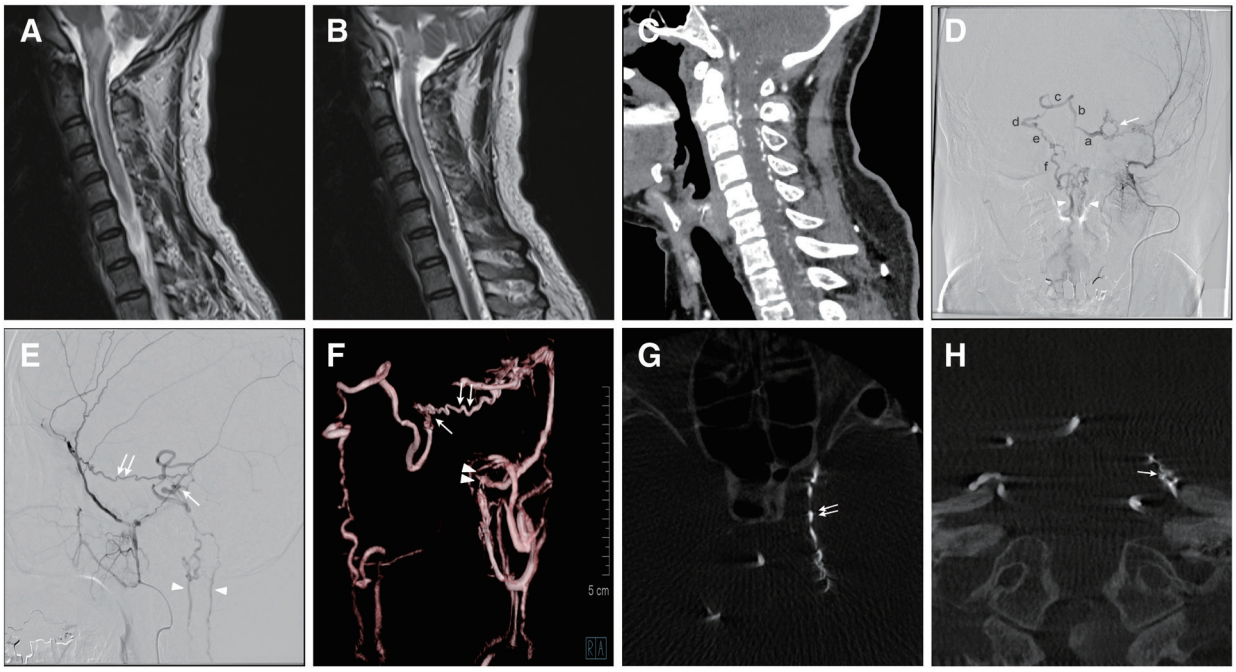

Fig. 1 (**A, B**) Sagittal sections of MRI (two consecutive slices) showing the T2-hyperintensity and swelling in the brainstem and spinal cord from the medulla oblongata to vertebral level C6 with perimedullary vascular flow voids. (**C**) The sagittal section of CTA more clearly shows the tortuous and dilated vessels around the cervical spine. (**D**, **E**) Superselective angiograms of the left MMA. Anterior-posterior view (**D**) and lateral view (**E**). A single feeder from a sphenoid branch of the left MMA connects with the marginal tentorial artery (double white arrows) and runs toward the fistula point (single white arrow) on the top of the left petrous ridge, draining into a left petrosal vein. A drainer (a left petrosal vein) connects to a left transverse pontine vein (a), a median anterior pontomesencephalic vein (b), a right transverse pontine vein (c), a right petrosal vein (d), a right lateral pontine vein (e), and a right lateral medullary (f). These abnormal venous drainages finally connect to anterior and posterior spinal veins (white arrowheads). (**F–H**) The oblique view of 3DRA of the left MMA and its source images (axial and coronal sections). These images clearly show the MMA feeder connecting with a marginal tentorial artery (double arrows) that runs toward the shunt point (single arrow) on the top of the left petrous ridge. Double arrowheads indicate the foramen spinosum. MMA, middle meningeal artery; 3DRA, three-dimensional rotational angiography

disturbance, left-sided numbness, increased bilateral patellar tendon reflexes, and urinary retention. MRI showed the T2-hyperintensity from the medulla oblongata to C6 with vascular flow voids, suggesting underlying arteriovenous shunts between the craniocervical junction and the upper cervical spine (**Fig. 1A** and **1B**). Cervical CTA more clearly revealed abnormal spinal veins around the spinal cord (**Fig. 1C**). Based on MRI and CTA findings, an upper cervical spinal arteriovenous fistula (AVF) was suspected. Unexpectedly, cerebral angiography revealed a tentorial DAVF, which was supplied by the left middle meningeal artery (MMA) and drained directly into the left petrosal vein (**Fig. 1D** and **1E**). The venous drainage system was connected to the anterior and posterior spinal veins via a complex venous network composed of several brainstem veins and a contralateral (right) petrosal vein. The patient was diagnosed with tentorial DAVF with spinal perimedullary venous drainage (Cognard type V). 3D rotational angiography revealed that a single feeder from the sphenoid branch of the MMA connected with the marginal tentorial artery that ran toward the distant shunt point located on the top of the left petrous ridge (**Fig. 1F–1H**). In cases such as this, direct surgery (DS) was considered preferable to endovascular treatment (EVT). The patient underwent a lateral suboccipital craniotomy and microsurgical dissection via the lateral supracerebellar–infratentorial route using a retrosigmoid approach. An arterialized drainer (left petrosal vein) hanging from the lateral inferior side of the tentorium was identified (**Fig. 2A**). The connection between the target drainer and the tentorium was interrupted, and the drainer was normalized. Postoperative DSA revealed complete obliteration of the tentorial DAVF (**Fig. 2B** and **2C**). The interval from onset to fistula occlusion was 1 month. Six months after the operation, a follow-up MRI showed that the vascular flow voids and T2-hyperintensity between the medulla oblongata and cervical spinal cord had disappeared (**Fig. 2D**). His motor strength and bladder function improved significantly. Regarding sensory disturbances, the patient still experienced no interval changes.

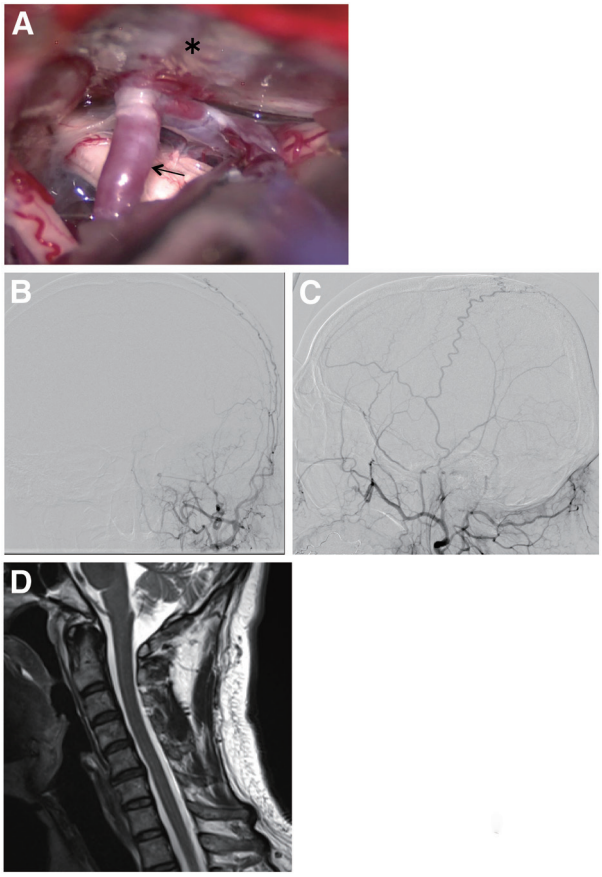

Fig. 2 (**A**) An intraoperative photograph shows an arterialized petrosal vein (black arrow) hanging from the lateral inferior side of the tentorium (asterisk). (**B, C**) Anterior–posterior view and lateral view in the left external carotid angiography show the complete occlusion of the tentorial dural arteriovenous fistula. (**D**) The sagittal section of the postoperative MRI shows that the T2-hyperintensity and the swelling in the brainstem and spinal cord have disappeared. The perimedullary vascular flow voids completely disappeared.

Case 2

A 47-year-old man visited the neurology department of our institution with a 6-month history of a progressive tingling sensation in both lower limbs and decreased urinary and fecal sensation. During the neurological examination, the patient reported a tingling sensation in the hips, feet, lower legs, and thighs. Spastic gait and hyperreflexia of the lower limbs were also observed. No motor weakness, sensory disorders (pain, light touch, or position sense), or pathological reflexes were observed. Head MRI and MRA did not reveal any abnormal findings. Spinal MRI revealed swelling and T2-hyperintensity in the cervical spinal cord from vertebral levels C1 to C7 (**Fig. 3A**). Vascular flow voids were not observed around the spinal cord. Although tortuous flow voids were observed in the dorsal side to the medulla oblongata, we considered the higher possibility of the normal posterior inferior cerebellar artery (PICA) than that of abnormal vessels. Myelitis was suspected, and immunological, cerebrospinal fluid, and contrast-enhanced MRI tests were performed. Immunoserological tests were negative, and a cerebrospinal fluid test revealed albuminocytologic dissociation. Contrast-enhanced MRI revealed a long and faint patchy gadolinium enhancement in the spinal cord from the C3 to C5 vertebral levels, with vascular enhancement (**Fig. 3B** and **3C**). Despite the long clinical course of 6 months and obvious MRI findings of longitudinal T2-hyperintensity, the mild clinical symptoms were thought to be atypical for myelitis. To exclude spinal AVF, cervical CTA was performed, and abnormal vessels around the spinal cord surface were identified (**Fig. 3D**), indicating congestive myelopathy due to arteriovenous shunt disease. Although arteriovenous shunt disease between the craniocervical junction and cervicothoracic spine was suspected, cerebral angiography unexpectedly identified a foramen magnum DAVF with spinal perimedullary venous drainage (Cognard type V). The feeders were the dilated jugular branch of the right ascending pharyngeal artery (AphA) and the dural branch of the right vertebral artery (VA) (**Fig. 3E–3I**). A single drainer arising from the fistula of the foramen magnum entered the spinal veins (**Fig. 3F, 4A,** and **4B**). We thought that a microcatheter could reach close to the shunt point through a dilated jugular branch of the right AphA and decided to perform transarterial embolization (TAE) of the foramen magnum DAVF. After proximal embolization of the VA feeder using coils (**Fig. 4C** and **4D**), a DeFrictor Nano Catheter (Medico's Hirata, Osaka, Japan) was navigated to the jugular branch of the right AphA, close to the shunt point (**Fig. 4D**). N-butyl-2-cyanoacrylate (17%) was injected, and the glue penetrated the venous pouch through the fistula (**Fig. 4E**). The final angiogram showed the disappearance of the foramen magnum DAVF. Postoperative MRI showed resolution of the spinal cord enlargement and a gradual decrease in T2-hyperintensity (**Fig. 4F**). The interval between the onset and fistula occlusion was 7 months. One year after treatment, his gait disturbance improved significantly, but he still experienced tingling in his lower extremities and occasional urinary incontinence.

Discussion

Intracranial DAVFs with perimedullary venous drainage, also called CVDFs, are rare. Cognard et al.[2] reported CVDFs in 12 of 205 patients with intracranial DAVFs. They also reported that six patients (50%) presented

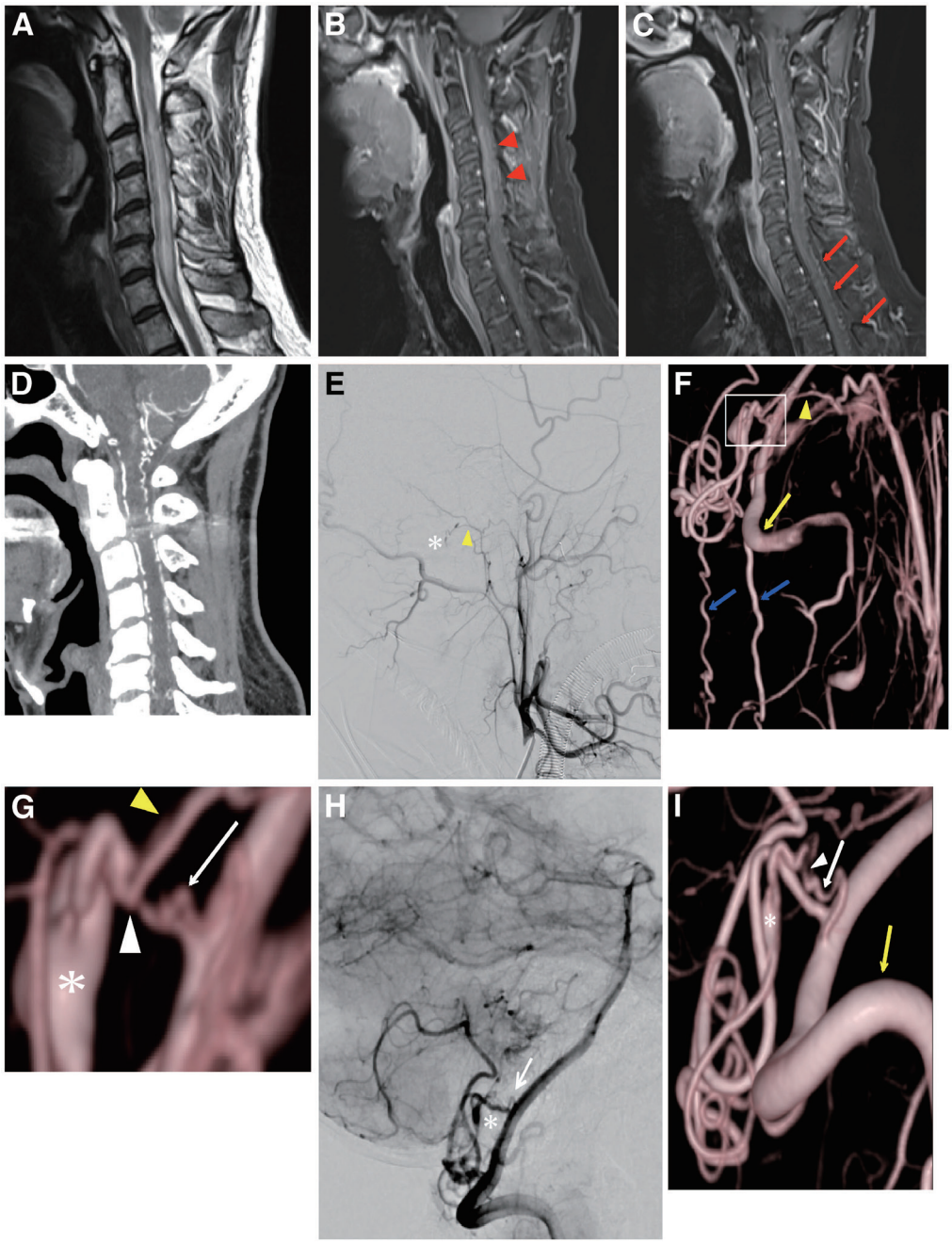

Fig. 3 (**A**) Spinal MRI revealing the T2 hyperintensity and the swelling of the cervical spinal cord from C1 to C7 vertebral levels. The vascular flow voids around the spinal cord surface are not obviously identified. Tortuous flow voids in the dorsal side to the medulla oblongata are observed, which was considered to be the normal PICA. (**B, C**) A contrast-enhanced MRI showed a long, faint, patchy Gd enhancement (red arrowheads) in the spinal cord from vertebral levels C3 to C5 with abnormal vascular enhancement (red arrows). (**D**) The sagittal section of cervical CTA shows abnormal vessels around the spinal cord surface, indicating congestive myelopathy due to arteriovenous shunt disease. (**E–G**) Lateral view of DSA from a right external carotid artery (**E**). Posterolateral view of 3DRA of the right AphA (**F**). The magnified image (**G**) of the white square frame of **F**. These images show the angioarchitecture of the AphA feeder (**E–G**, yellow arrowhead), VA feeder (white arrow), fistula (white arrowhead), and venous pouch (**E** and **G**, asterisk). A feeder (**E–G**, yellow arrowhead) supplied from a dilated jugular branch of the right AphA shows the caliber change at the fistula (white arrowhead). After draining from the fistula point, it formed a venous pouch (**E** and **G**, asterisk) and then finally connected to an anterior and a posterior spinal vein (blue arrows). This 3DRA image (**F**) also shows a right VA was retrogradely depicted via a VA feeder through the same fistula point. (**H, I**) Lateral view of DSA (**H**) and 3DRA (**I**) from a right vertebral artery. These images reveal another feeder (white arrow) supplied from a right VA (yellow arrow) running into the same fistula point (white arrowhead) and venous pouch (**H** and **I**, asterisk). AphA, ascending pharyngeal artery; PICA, posterior inferior cerebellar artery; VA, vertebral artery; 3DRA, three-dimensional rotational angiography

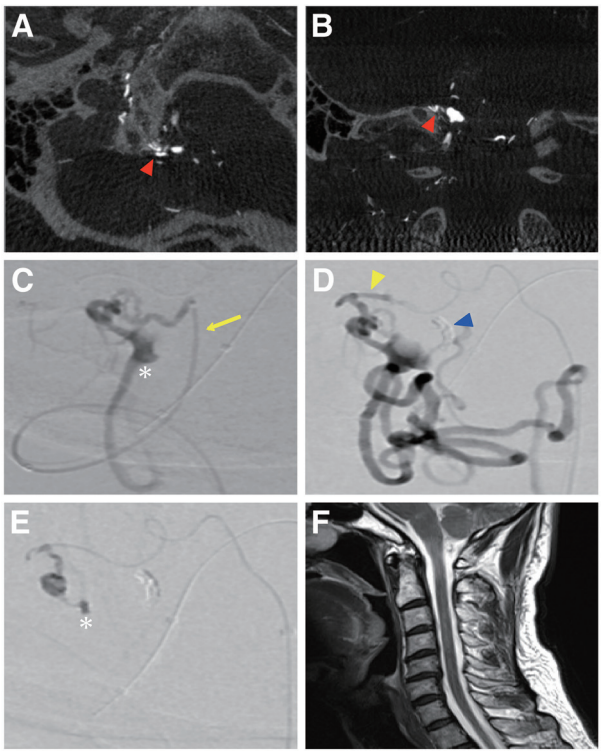

Fig. 4 Axial (**A**) and coronal (**B**) 3DRA source images of a right AphA demonstrating that the fistula point (red arrowhead) is located on the medial side of the right jugular tubercle. Superselective angiograms (**C–E**) are the same working angle views. (**C**) An Excelsior SL-10 microcatheter (Stryker, Kalamazoo, MI, USA) was navigated into a right VA feeder (yellow arrow). The asterisk indicates a venous pouch. A DeFrictor Nano Catheter was navigated into the distal portion of a jugular branch from the right AphA. (**D**) After the placement of coils (blue arrowhead indicates the digital-subtracted coil mass) in the VA feeder, superselective angiography from a DeFrictor Nano Catheter demonstrates that the retrograde depiction of a right VA main trunk is not confirmed (yellow arrowhead, AphA feeder). (**E**) 17% n-butyl-2-cyanoacrylate was injected from a DeFrictor Nano Catheter, and the glue slightly penetrated the venous pouch (asterisk) through the fistula. DSA from a right VA and a right common carotid artery show the disappearance of foramen magnum DAVF (not shown). The sagittal section of the postoperative MRI (**F**) shows that the T2-hyperintensity and swelling in the cervical spinal cord decreased. AphA, ascending pharyngeal artery; DAVF, dural arteriovenous fistula; VA, vertebral artery; 3DRA, three-dimensional rotational angiography

with progressive myelopathy, and five patients (41.7%) presented with subarachnoid hemorrhage. Haryu et al.[4] analyzed 57 cases of CVDFs and revealed that the onset of CVDFs was mainly due to progressive myelopathy symptoms and, less frequently, subarachnoid hemorrhage. Although the fistula locations of CVDFs are remote intracranial regions, myelopathy symptoms and MRI T2-hyperintensity of the spinal cord strongly suggest spinal lesions. Therefore, myelopathy caused by CVDFs is often difficult to diagnose.[1,3,5–8] We systematically reviewed the literature to investigate the clinical characteristics and disadvantages of CVDFs. Using the PubMed database, we retrieved four case reports,[1,5,7,9] three case series,[2,4,8] and one review article[3] written in English using the terms "myelopathy," "intracranial dural arteriovenous fistula," and "Cognard Type V." In addition, regarding the fistula sites, we excluded cases treated as "cranio-cervical junction" and "not available" because both types were not precisely identified as intracranial DAVFs. Finally, the literature review included papers published since 1988 and identified 88 patients diagnosed with CVDFs with myelopathy onset (**Table 1**).[1–5,7–9] The median and mean ages of the patients were 60 and 55.8 years, respectively. There were 65 males (73.9%) and 23 females (26.1%). All the patients presented with congestive myelopathy. The percentage of patients correctly diagnosed with intracranial DAVFs was 29.5%. The most common initial misdiagnosis was myelitis (27.3%), followed by spinal DAVFs (14.8%) and neoplasms (9.1%). This was also true for our cases, as we initially suspected a spinal AVF in Case 1 and myelitis in Case 2. The median and mean diagnostic delays (intervals from onset to definite diagnosis) were 6 and 9 months, respectively. The diagnosis of CVDFs is difficult, leading to potential diagnostic delays and poor neurological recovery.[3,10] On conventional spinal MRI, there are no specific radiological signs of CVDFs except for predominant vascular flow voids around the brain stem in addition to the cervical spinal cord. Even if some neurologists may notice the vascular flow voids around the cervical spinal cord, they tend to suspect spinal (extracranial) DAVFs. However, spinal angiography, including bilateral vertebral angiography cannot often detect the CVDFs.[11] Several studies have reported that contrast-enhanced MR imaging and CTA could make abnormal perimedullary vessels more obvious about faintly dilated veins around the brain stem and the cervical spine.[4,7,8,12] In particular, the abnormal dilated veins around the brain stem were reported to suggest the CVDFs.[13] As shown in case 2, I thought retrospectively that I should have speculated the flow voids dorsal to the medulla oblongata to be abnormal vessels. Nonetheless, the source CTA images were very helpful in detecting faintly dilated veins around the brain stem and the cervical spine. Therefore, we considered the possibility of not only spinal DAVFs but also intracranial DAVFs and performed common carotid angiography in addition to vertebral and spinal angiography, which finally led to a correct diagnosis in a short time from the first treatment visit.

Subsequently, we investigated the reports of the breakdown of fistula sites in CVDFs through the literature review (**Table 1**).[1–5,7–9] There is a lack of terminological

Table 1 Summary of the literature review regarding Cognard type V dural arteriovenous fistulas

Characteristics	Value
Total number of patients	88
Age	
Median/mean	60/55.8
Sex	
Male/female	65/23
MRI findings (without contrast agents)	
T2 hyperintensity of brainstem and spinal cord	88 (100%)
No vascular flow void around the spinal cord	11 (12.5%)
Initial diagnosis (Correct)	
Intracranial DAVF	26 (29.5%)
Initial diagnosis (wrong)	
Myelitis	24 (27.3%)
Spinal DAVF	13 (14.8%)
Neoplasm	8 (9.1%)
Stroke	6 (6.8%)
Others	Trauma 1, Spinal canal stenosis 1, NA 17
The interval from onset to definite diagnosis	
Median/mean	6/9 months
Fistula site (N = 88)	
Petrous/tentorial region	50 (56.8%)
Foramen magnum region	19 (21.6%)
Transverse-sigmoid sinus	10 (11.4%)
Torcular herophili	3 (3.4%)
Suboccipital convexity dura/occipital sinus	3 (3.4%)
Others	CS 2, ACF 1
Treatment (N = 81)	
DS (initial treatment)	28 (34.6%)
EVT (initial treatment)	53 (65.4%)
DS (salvage treatment after failed EVT)	15
Approach routes and embolic materials of EVT (N = 51)	
TAE 46 (liquid only 32, liquid + particle 2, particle only 7, NA 5)	
TVE 5 (coil only 4, coil + liquid 1)	
Outcome (N = 74)	
Good recovery	24 (32.4%)
Moderate disability	27 (36.5%)
Severe disability/death	23 (31.1%)

"Good recovery" indicates the complete regression of symptoms.
"Moderate disability" indicates the ability to walk with support and live independently despite the neurologic sequelae interfering with daily activities.
"Severe disability/death" indicates the inability to walk and requiring nursing care due to neurologic sequelae severely interfering with daily activities or death.
ACF, anterior cranial fossa; CS, cavernous sinus; DAVF, dural arteriovenous fistula; DS, direct surgery; EVT, endovascular treatment; NA, not available; TAE, transarterial embolization; TVE, transvenous embolization

consistency regarding the locations of the fistulas reported in each study. For convenience, we grouped the petrous ridge, superior petrosal sinus, and tentorium as the petrous ridge/tentorial regions. In addition, based on a previous study,[14,15] we grouped the foramen magnum and surrounding areas (jugular tubercle, anterior condylar confluence, anterior condylar vein, posterior condylar vein, marginal sinus, and jugular foramen) as the foramen magnum regions. As a result, we found that the most common region was the petrous ridge/tentorial region (56.8%), followed by the foramen magnum region (21.6%) and the transverse-sigmoid sinus (11.4%), which resembled our cases. Of the 88 patients, 81 underwent treatment for CVDFs. As initial treatment, DS was performed in 28 patients (34.6%), and EVT was performed in 53 patients (65.4%). However, of the 53 patients treated with EVT on the first attempt, 15 underwent DS as a salvage therapy after failed fistula embolization. Of 53 patients treated with EVT, the details of endovascular approach routes were available in 51 patients. About 90% (46/51) of patients

treated with EVT were performed by TAE. As the embolic materials used with TAE, liquid agents accounted for about 74% (34/46). By contrast, only five patients were performed by transvenous embolization (TVE). Of five patients treated with TVE, the locations of DAVFs were four patients with the transverse-sigmoid sinus DAVFs and one patient with the petrous ridge/tentorial region DAVF (superior petrosal sinus). Regarding the outcome after the treatment of CVDFs, our literature review revealed that 67.6% of patients with CVDFs had residual myelopathy symptoms, while the remaining 32.4% achieved full recovery.

Conclusion

Spinal cord surface flow voids are not always obvious in CVDFs, despite the fact that they have caused venous congestion (T2-hyperintensity and swelling) in the cervical spinal cord. However, in such cases, it is important not to miss any only minor vascular flow voids around the brainstem and the cervical spinal cord. Contrast-enhanced MRI and CTA can be useful for visualizing abnormal vessels around the brainstem and spinal cord. The co-presence of the abnormal vessels around the brain stem can suggest the CVDFs. Not only spinal DAVFs but also CVDFs should be considered as the differential diagnoses for venous congestive cervical myelopathy, in which cases cerebral angiography including carotid angiography is essential.

Patient Consent

Consent from the patient was obtained.

Disclosure Statement

The authors declare that they have no conflicts of interest.

References

1) Cobos Codina S, Bernal García LM, Rodríguez Sánchez JA, et al. Tentorial dural arteriovenous fistula with perimedullary venous drainage-associated cervical myelopathy: illustrative case. *J Neurosurg Case Lessons* 2022; 4: CASE22148.
2) Cognard C, Gobin YP, Pierot L, et al. Cerebral dural arteriovenous fistulas: clinical and angiographic correlation with a revised classification of venous drainage. *Radiology* 1995; 194: 671–680.
3) De Grado A, Manfredi C, Brugnera A, et al. Watch brain circulation in unexplained progressive myelopathy: a review of Cognard type V arterio-venous fistulas. *Neurol Sci* 2023; 44: 3457–3480.
4) Haryu S, Endo T, Sato K, et al. Cognard type V intracranial dural arteriovenous shunt: case reports and literature review with special consideration of the pattern of spinal venous drainage. *Neurosurgery* 2014; 74: E135–E142; discussion, E142.
5) Jermakowicz WJ, Weil AG, Vlasenko A, et al. Cognard Type V intracranial dural arteriovenous fistula presenting in a pediatric patient with rapid, progressive myelopathy. *J Neurosurg Pediatr* 2017; 20: 158–163.
6) Bernard F, Lemée JM, Faguer R, et al. Lessons to be remembered from a dural arteriovenous fistula mimicking medulla and high cervical cord glioma. *World Neurosurg* 2018; 113: 312–315.
7) Roelz R, Van Velthoven V, Reinacher P, et al. Unilateral contrast-enhancing pontomedullary lesion due to an intracranial dural arteriovenous fistula with perimedullary spinal venous drainage: the exception that proves the rule. *J Neurosurg* 2015; 123: 1534–1539.
8) Whittam D, Huda S, Gibbons E, et al. A case series of intracranial dural arteriovenous fistulae mimicking cervical myelitis: a diagnosis not to be missed. *J Neurol* 2021; 268: 4680–4686.
9) Rubio RR, Chae R, Rutledge WC, et al. Clipping of high-risk dural arteriovenous fistula of the posterior fossa: 3-dimensional operative video. *World Neurosurg* 2019; 126: 413.
10) Wiesmann M, Padovan CS, Pfister HW, et al. Intracranial dural arteriovenous fistula with spinal medullary venous drainage. *Eur Radiol* 2000; 10: 1606–1609.
11) van Rooij WJ, Sluzewski M, Beute GN. Intracranial dural fistulas with exclusive perimedullary drainage: the need for complete cerebral angiography for diagnosis and treatment planning. *AJNR Am J Neuroradiol* 2007; 28: 348–351.
12) Kim NH, Cho KT, Seo HS. Myelopathy due to intracranial dural arteriovenous fistula: a potential diagnostic pitfall. *J Neurosurg* 2011; 114: 830–833.
13) Li J, Ezura M, Takahashi A, et al. Intracranial dural arteriovenous fistula with venous reflux to the brainstem and spinal cord mimicking brainstem infarction. *Neurol Med Chir (Tokyo)* 2004; 44: 24–28.
14) Li C, Yu J, Li K, et al. Dural arteriovenous fistula of the lateral foramen magnum region: a review. *Interv Neuroradiol* 2018; 24: 425–434.
15) Hiramatsu M, Ozaki T, Aoki R, et al. Non-sinus-type dural arteriovenous fistula at the foramen magnum: a review of the literature. *J Neuroendovasc Ther* 2023 July 12. 2023. doi.org/10.5797/jnet.ra.2023-0019. [Epub ahead of print].